Available online at www.sciencedirect.com
SCIENCE DIRECT
ELSEVIER
Journal of the European Ceramic Society 26 (2006) 1921–1924
ECERS
www.elsevier.com/locate/jeurceramsoc

Probing point defects in $Ba(B'_{1/3}B''_{2/3})O_3$ by ESR, PAS and dielectric spectroscopy

T. Kolodiazhnyi [a,*], G. Annino [b], A. Younker [c], P. Malysz [c], P. Mascher [c], H. Haneda [a]

[a] *National Institute for Materials Science, Tsukuba, Ibaraki 305-0044, Japan*
[b] *Institute for Chemical and Physical Processes, Pisa 56124, Italy*
[c] *Department of Engineering Physics, McMaster University, Hamilton, Ont., Canada L8S 4L7*

Available online 17 October 2005

Abstract

In contrast to simple ternary perovskites (e.g., $SrTiO_3$ and $BaTiO_3$), the defect chemistry model of complex barium perovskites with general formula $Ba(B'_{1/3}B''_{2/3})O_3$ has yet to be developed. In an attempt to gain an insight into a point defect chemistry of these compounds, we present first results of electron spin resonance, positron annihilation spectroscopy and dielectric spectroscopy (10–100 GHz) of $Ba(B'_{1/3}B''_{2/3})O_3$, where B′ = Mg, Zn, Ni, Co and B″ = Nb and Ta. Both extrinsic and intrinsic defects were found in these materials. A Mn ion impurity serves as an excellent sensor for the early stages of the B-site cation disorder and oxygen activity. Based on the several $Ba(B'_{1/3}B''_{2/3})O_3$ examples, we demonstrate that Schottky disorder plays a crucial role in the high temperature phase stability and dielectric loss of $Ba(B'_{1/3}B''_{2/3})O_3$ perovskites.

Keywords: Perovskites; Defects; Spectroscopy; Dielectric properties; Magnetic properties

1. Introduction

Over the last 30 years, considerable research activity was dedicated to the origin of the dielectric loss in the low-loss microwave dielectrics.[1] As revealed by the FIR spectroscopy[1] and latter confirmed by the microwave studies at cryogenic temperatures,[2] the major contribution to the dielectric loss of commercial low-loss dielectric ceramics has an extrinsic origin. In other words, in most cases, the losses due to the crystal imperfections (e.g., lattice disorder, point defects, dislocations, grain boundaries, second phase) dominate over intrinsic loss due to the two-phonon-difference absorption.[3] Although preliminary results on the crystal imperfections are traditionally obtained by the standard analytical tools, such as XRD, SEM and TEM, the analysis of the point defects and lattice disorder at the ppm level in the high-Q dielectric ceramics obviously requires a novel approach.

Unlike the simple ternary $A^{2+}B^{4+}O_3$ perovskites, the point defect chemistry of the complex $Ba(B'_{1/3}B''_{2/3})O_3$ perovskites is largely unknown. However, taking into account a densely packed perovskite structure, the Frenkel defects are usually ignored and only Schottky disorder is considered. The first-principles calculations show that the 1:2 ordering of the B-site cations along the ⟨1 1 1⟩ directions minimizes the concentration of the underbounded oxygens in the B′–O–B′ environments.[4] The 1:2 ordering also leads to the expansion of the $B'O_6$ octahedron and contraction of the $B''O_6$ octahedron.[5] The calculated density of states (DOS) indicates some degree of covalent bonding between the oxygens and the B″ cations whereas the O–B′ bonds remain purely ionic.[6] The difference in the effective charges of the B-site cations and their bonding to oxygens in the $Ba(B'_{1/3}B''_{2/3})O_3$ compounds would result in quite different formation energies of the B′ and B″ vacancies. In thermodynamic equilibrium, the concentration of these defects would increase exponentially with temperature.[7] There is a high probability that some of these vacancies will have an unpaired electron spin, thus making them ESR-active. Hence, by applying spin-sensitive techniques, it would be possible to detect and characterize trace amounts of these lattice defects. In this contribution, we outline several methods of analysis of the early stages of the lattice disorder in the $Ba(B'_{1/3}B''_{2/3})O_3$ complex perovskites.

2. Experiment

Samples of compositions given in Table 1 were prepared by a solid-state method from metal oxides and carbonates of

* Corresponding author. Tel.: +81 29 851 3354.
E-mail address: kolodiazhnyi.taras@nims.go.jp (T. Kolodiazhnyi).

0955-2219/$ – see front matter © 2005 Elsevier Ltd. All rights reserved.
doi:10.1016/j.jeurceramsoc.2005.09.022

Table 1
Positron lifetime data of the $Ba(B'_{1/3}B''_{2/3})O_3$ compounds

Symbol	τ_1 (ps)	τ_D (ps)	I_D (%)	τ_{av} (ps)	τ_b (ps)	κ (ns^{-1})
BNT	164	292	27	201	186	0.727
BNN	166	300	30	208	191	0.808
BMT	183	317	34	231	214	0.792
BMN	182	303	27	217	205	0.595
BZT	159	280	46	217	198	1.25
BZN	183	273	36	218	208	0.653

99.99% purity. The mixtures were calcined at 950–1200 °C in air for 20 h. The obtained powders were milled for 24 h, pressed into pellets and sintered at 1290–1700 °C in air or forming gas (7% H_2/93% Ar). Dielectric properties were measured at 10 GHz ($TE_{01\delta}$ mode) using HP 8510 vector network analyzer and at 20–100 GHz (WGE and WGH whispering gallery modes) using an ABmillimetre vector network analyzer. The whispering gallery modes (WGM) technique employed for the dielectric characterization of the samples is an extension of the approach discussed in reference.[8] A detailed analysis of this millimeter wave WGM spectroscopy will be presented elsewhere. Magnetic susceptibility of selected samples was measured in the 5–300 K range by means of superconducting quantum interference device, SQUID (Quantum Design). The electron spin resonance (ESR) studies were performed on Bruker ELEXSYS E580 X-band ESR spectrometer (courtesy of Bruker-Biospin, Tsukuba). For comparative ESR analysis, the weight of the powdered samples was kept at 50 ± 0.1 mg. The measurements were performed in the frequency range of 9.8–9.9 GHz at a constant microwave power of 2 mW. Positron annihilation spectroscopy (PAS) was carried out using a conventional fast-fast lifetime spectrometer with a time resolution (FWHM) of 240 ps. A 30 mCi ^{22}Na positron source was used in a conventional Al-foil arrangement. Each spectrum contained 6×10^6 counts and was analyzed using the program POSITRONFIT. The data presented in Table 1 are averages of typically four separate runs.

3. Results and discussion

It is accepted that the lowest limit of the dielectric loss at the microwave (MW) frequency (10 GHz) can be estimated from the extrapolation of the $\tan\delta$ from the far infrared.[9] It is speculated that this method allows fast screening of the DR candidates bypassing a time consuming optimization of ceramics. However, this approach suffers from the two major drawbacks. First, it appears to be not accurate enough due to the extrapolation over the 2–3 decades of frequency, and second, it still requires well processed ceramics with negligible extrinsic dielectric loss at the far infrared.[10]

Fig. 1 shows frequency dependence of the room temperature dielectric properties, i.e. ε and $\tan\delta$ of $Ba(Mg_{1/3}Ta_{2/3})O_3$ (BMT) ceramics. The MW and millimeter data were obtained from the same dielectric material. The SMM data of Murata ceramics at 300 GHz were taken from reference.[10] As revealed from our millimeter data obtained from the whispering gallery

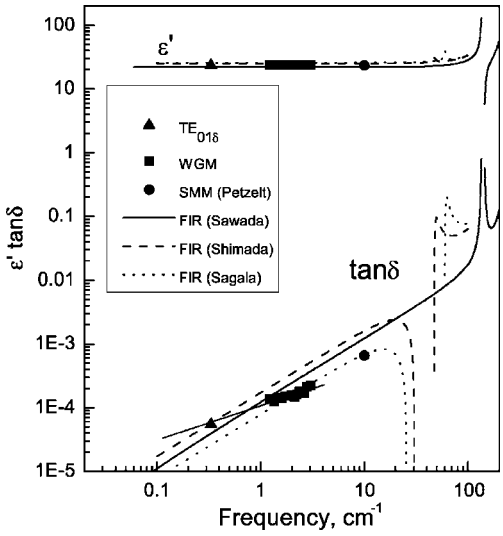

Fig. 1. Room temperature ε' and $\tan\delta$ of $Ba(Mg_{1/3}Ta_{2/3})O_3$. The SMM data are from reference.[10] The FIR data are from references.[11–13]

dielectric resonator, the change in the slope of the $\tan\delta$ versus frequency from 0.49 to 1.0 at ca. 70–80 GHz indicates that intrinsic dielectric loss in the well processed $Ba(Mg_{1/3}Ta_{2/3})O_3$ takes over extrinsic one above 80 GHz. Extrapolation of the FIR data of Sagala[12] down to the 10–300 GHz seems to agree fairly well with both the sub-millimeter data of Petzelt[10] and our millimeter data of the $WGH_{n,0,0}$ whispering gallery modes, where $3 \leq n \leq 15$. The only disadvantage of the factorized representation of the dielectric function is an erroneous (negative) value of the $\tan\delta$ that often appears in the part of the extrapolated region.[12,13]

With an exception of the Ni- and Co-containing dielectric resonators that show strong paramagnetism, the rest of the dielectrics studied here are normally diamagnetic. Any deviation from the temperature independent diamagnetic behavior would indicate that the material contains lattice defects with a non-zero magnetic moment. The effect of sintering temperature on the molar magnetic susceptibility, χ_m of $Ba(Mg_{1/3}Ta_{2/3})O_3$ is shown in Fig. 2. A strong temperature-dependent contribution to

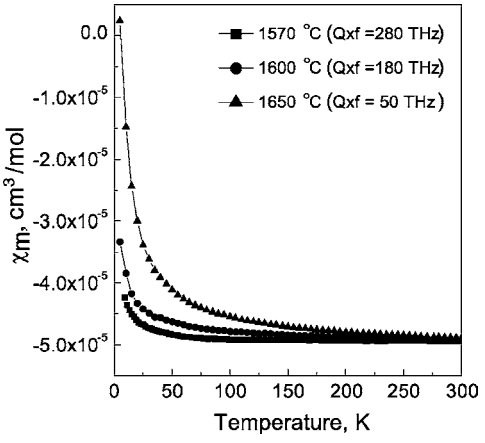

Fig. 2. Effect of processing temperature on the molar magnetic susceptibility of $Ba(Mg_{1/3}Ta_{2/3})O_3$.

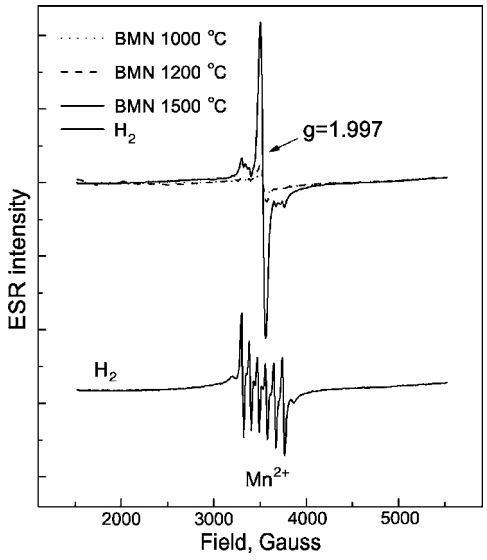

Fig. 3. Room temperature ESR spectra of $Ba(Mg_{1/3}Nb_{2/3})O_3$ processed at various temperatures. The spectrum of the BMN annealed in the forming gas is shifted down for clarity.

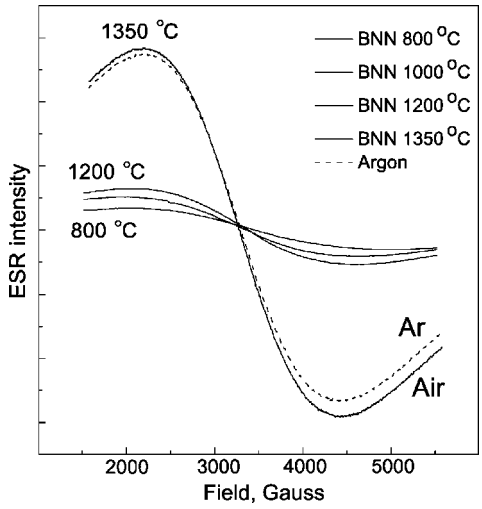

Fig. 4. Room temperature ESR spectra of $Ba(Ni_{1/3}Nb_{2/3})O_3$ processed at various temperatures and atmospheres.

the χ_m comes from the paramagnetic lattice defects at the low-temperatures. The concentration of the lattice defects increases exponentially with processing temperature and so does the low-temperature χ_m. At sufficiently high temperatures, χ_m levels off at ca. -49.6×10^{-6} cm^3/mol. The calculated molar magnetic susceptibility[14] of BMT is -78.3×10^{-6} cm^3/mol which is significantly lower than the measured value. This result is in accord with the first-principles calculations[6] showing that the purely ionic picture of BMT is not valid and some covalent bonding between the O-2p and Ta-5d orbitals generate additional paramagnetic contribution to the χ_m.

The room temperature ESR signals associated with the paramagnetic lattice defects were detected in all but $Ba(Co_{1/3}Nb_{2/3})O_3$ samples. The BMT and BMN spectra showed a qualitatively similar behavior and only the ESR spectra of BMN are discussed here. The effect of processing temperature and the annealing atmosphere on the ESR spectra of the BMN is shown in Fig. 3. There is a progressive increase of the ESR singlet with a giromagnetic constant of $g = 1.997$ as a processing temperature increases from 1000 to 1500 °C. Development of the $g = 1.997$ signal is also accompanied by the appearance of the Mn^{2+} sextet in the spectra. Mn was present as a trace impurity in the precursors. Annealing of BMN in the forming gas removes the central ESR feature and also significantly enhances the Mn^{2+} signal. At high oxygen partial pressure, Mn has an oxidation state of +4 and occupies the B″ sites of the $Ba(B'_{1/3}B''_{2/3})O_3$ compounds. An increase in the Mn^{2+} signal at higher processing temperatures indicates that Mn starts to substitute the B′ cation. High-temperature reduction of ceramics at low oxygen partial pressure further increases the concentration of Mn^{2+} via the formation of the $[Mn^{2+}_{Nb}V_{\ddot{O}}]$ complex. The paramagnetic center with $g = 1.997$ is ascribed to the lattice defect with a trapped hole. Upon reduction of ceramics, the $g = 1.997$ signal disappears due to the upward shift of the Fermi level. Our preliminary study on the non-stoichiometric BMN indicates that the $g = 1.997$ signal is associated with a singly ionized barium vacancy.

The ESR spectra of the Mott-Hubard insulators, BNT and BNN, revealed somewhat different behavior of the lattice defects. In the case of BNN, strong and broad ESR signal associated with the Ni^{3+} impurity progressively increases with processing temperature from 800 to 1350 °C (Fig. 4). In contrast to BNN, the relatively weak Ni^{3+} signal increases in BNT only up to $T \approx 1400$ °C (Fig. 5). At higher processing temperature, the Ni^{3+} signal decreases which is accompanied by the appearance of a new singlet at $g = 2.000$. Obviously, the $g = 2.000$ lattice defect that develops at higher temperatures suppresses the concentration of Ni^{3+} in BNT. This may partially explain much higher Q-values of the BNT as compared to the BNN.[15] More results on the ESR spectroscopy of the $Ba(B'_{1/3}B''_{2/3})O_3$ compounds will appear in a separate publication.

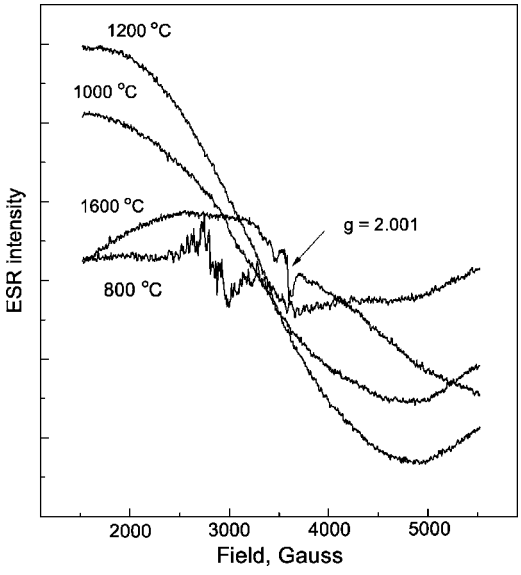

Fig. 5. Room temperature ESR spectra of $Ba(Ni_{1/3}Ta_{2/3})O_3$ processed at various temperatures.

The positron annihilation relies on the fact that positrons become trapped at neutral and negative vacancies due to the missing positive charge of the ion cores. The reduced valence and core electron densities at vacancies increase the positron lifetime and narrow the positron–electron momentum distribution. Although it is quite difficult to decompose the positron lifetime spectra for a multi-defect systems, our PAS data show the presence of significant amount of vacancy defects in all studied $Ba(B'_{1/3}B''_{2/3})O_3$ compounds (see Table 1). According to the PAS data, the zinc containing compounds show the largest concentration of the open volume lattice defects (I_D = 46% for BZT and I_D = 36% for BZN). The BZT also shows the highest trapping rate ($\kappa = 1.25\,ns^{-1}$). As expected, the bulk positron lifetime of the $Ba(B'_{1/3}B''_{2/3})O_3$ compounds increases linearly with the square root of the lattice constant from 186 to 208 ps with the only exception of the BMT. More accurate determination of the PAS parameters for non-stoichiometric samples is under way.

In conclusion, we have demonstrated that the early stages of the lattice disorder in the $Ba(B'_{1/3}B''_{2/3})O_3$ compounds, where the concentration of the lattice defects is still at the ppm level, can be detected and characterized by the several highly sensitive techniques including SQUID, ESR and PAS. We found that all studied compounds contain substantial amount of the lattice vacancy defects, some of them containing unpaired electron spin. The absence of the room temperature ESR signal in the $Ba(Co_{1/3}Nb_{2/3})O_3$ compound may be attributed to the short spin–spin relaxation time.

Acknowledgments

T.K. thanks Dr. T. Shimada for providing FIR fitting parameters of the BMT sample. Part of this study was performed through Special Coordination Funds for Promoting Science and Technology from the Ministry of Education, Culture, Sports, Science and Technology of the Japanese Government.

References

1. Petzelt, J. and Setter, N., Far infrared spectroscopy and origin of microwave losses in low-loss ceramics. *Ferroelectrics*, 1993, **150**, 89–102.
2. Alford, N. McN., Breeze, J., Wang, X., Penn, S. J., Webb, S. J., Ljepojevic, N. *et al.*, Dielectric loss of oxide single crystals and polycrystalline analogues from 10 to 320 K. *J. Eur. Ceram. Soc.*, 2001, **21**, 2605–2611.
3. Braginsky, V. B., Ilchenko, V. S. and Bagdassarov, Kh. S., Experimental observation of fundamental microwave absorption in high-quality dielectric crystals. *Phys. Lett. A*, 1987, **120**, 300–305.
4. Burton, B. P., Empirical cluster expansion models of cation order-disorder in $A(B'_{1/3}B''_{2/3})O_3$ perovskites. *Phys. Rev. B*, 1999, **59**, 6087–6091.
5. Desu, S. B. and O'Bryan, H. M., Microwave loss quality of $Ba(Zn_{1/3}Ta_{2/3})O_3$ ceramics. *J. Am. Ceram. Soc.*, 1985, **68**, 546–551.
6. Takahashi, T., Wu, E. J., Van Der Ven, A. and Ceder, G., First-principles investigation of B-site ordering in $Ba(Mg_x;Ta_{1-x})O_3$ microwave dielectrics with complex perovskite structure. *Jpn. J. Appl. Phys.*, 2000, **39**, 1241–1248.
7. Kingery, W., *Introduction to Ceramics*. J. Wiley & Sons, New York, 1976.
8. Annino, G., Bertolini, D., Cassettari, M., Fittipaldi, M., Longo, I. and Martinelli, M., Dielectric properties of materials using whispering gallery dielectric resonators: experiments and perspectives of ultra-wideband characterization. *J. Chem. Phys.*, 2000, **112**, 2308–2314.
9. Wakino, K., Murata, M. and Tamura, H., Far infrared reflection spectra of $Ba(Zn_{1/3}Ta_{2/3})O_3$–$BaZrO_3$ dielectric resonator material. *J. Am. Ceram. Soc.*, 1986, **69**, 34–37.
10. Petzelt, J. and Kamba, S., Submillimeter and infrared response of microwave materials: extrapolation to microwave properties. *Mater. Chem. Phys.*, 2003, **79**, 175–180.
11. Sawada, A. and Kuwabara, T., Infrared study of $Ba(Mg_{1/3}Ta_{2/3})O_3$ ceramics for microwave resonators. *Ferroelectrics*, 1989, **95**, 205–208.
12. Sagala, D. A. and Koyasu, S., Infrared reflection of $Ba(Mg_{1/3}Ta_{2/3})O_3$ ceramics. *J. Am. Ceram. Soc.*, 1993, **76**, 2433–2436.
13. Shimada, T., Dielectric loss damping constants of lattice vibrations in $Ba(Mg_{1/3}Ta_{2/3})O_3$ ceramics. *J. Eur. Ceram. Soc.*, 2003, **23**, 2647–2651.
14. Selwood, R. W., *Magnetochemistry*. Interscience Publishers, New York, 1956.
15. Kolodiazhnyi, T., Petric, A., Belous, A., V'yunov, O. and Yanchevskij, O., Synthesis and dielectric properties of barium tantalates and niobates with complex perovskite structure. *J. Mater. Res.*, 2002, **17**, 3182–3189.